Origin of odd-even staggering in fragment yields: Impact of nuclear pairing and shell structure on the particle-emission threshold energy

B. Mei,[1,2,3] H. S. Xu,[1,*] X. L. Tu,[1,2,4] Y. H. Zhang,[1] Yu. A. Litvinov,[1,2,4] K.-H. Schmidt,[2] M. Wang,[1] Z. Y. Sun,[1] X. H. Zhou,[1] Y. J. Yuan,[1] M. V. Ricciardi,[2] A. Kelić-Heil,[2] R. Reifarth,[3] K. Blaum,[4] R. S. Mao,[1] Z. G. Hu,[1] P. Shuai,[1,5] Y. D. Zang,[1] X. W. Ma,[1] X. Y. Zhang,[1] J. W. Xia,[1] G. Q. Xiao,[1] Z. Y. Guo,[1] J. C. Yang,[1] X. H. Zhang,[1] X. Xu,[1] X. L. Yan,[1,4] W. Zhang,[1] and W. L. Zhan[1]

[1]*Institute of Modern Physics, Chinese Academy of Sciences, Lanzhou 730000, China*

[2]*GSI-Helmholtzzentrum für Schwerionenforschung GmbH, D-64291 Darmstadt, Germany*

[3]*Goethe Universität Frankfurt, D-60438 Frankfurt am Main, Germany*

[4]*Max-Planck-Institut für Kernphysik, Saupfercheckweg 1, D-69117 Heidelberg, Germany*

[5]*University of Science and Technology of China, Hefei 230026, China*

(Received 3 November 2013; revised manuscript received 22 April 2014; published 19 May 2014)

Strong odd-even staggering (OES) of the yields of fragments, produced by fragmenting ^{78}Kr projectiles, has been measured by employing the combination of an in-flight fragment separator and a storage ring. It is shown that the OES of fragment yields of $T_z = -1/2$ and $T_z = 1/2$ mirror nuclei critically depends on both pairing and shell structure, especially at the closed shells $Z = 20$ and 28. A comparison of the relative OES of yields and of particle-emission threshold energies reveals unambiguously that the origin of the OES of fragment yields is mainly determined by the OES of the particle-emission threshold energies, which contain both pairing and shell effects.

DOI: 10.1103/PhysRevC.89.054612 PACS number(s): 25.70.Mn, 21.10.Dr, 21.30.Fe

I. INTRODUCTION

Nuclear reaction yields, especially fragmentation yields, can provide information on nuclear structure properties, e.g., pairing, shell effects, and densities of excited levels. Besides the straightforward application in nuclear structure, these nuclear properties are indispensable input data for modeling nucleosynthesis processes in stars and can have severe impact on the calculated element abundance distributions [1–3]. By themselves, fragmentation yields turn out to be sensitive probes for indicating the emergence of the island of inversion and investigating the evolution of shell structure [4,5], which is of basic interest, since new magic numbers may appear [6,7] and the known ones may disappear far from the valley of β-stability, due to, e.g., the contribution of tensor forces [8]. Fragmentation yields can also be used to study halo nuclei close to the drip lines [9].

Odd-even staggering (OES) has been observed in several of the most important quantities of nuclear physics, such as nuclear reaction yields [10,11], nuclear binding (separation) energies [12,13], and nuclear charge radii [14]. OES of fragment yields (OES-FY), that is, the enhancement in yields of even-Z nuclides compared with the neighboring odd-Z nuclides, has been intensively studied for different fragmentation reactions [9,11,15–34]. However, the existing experiments mainly concentrated on light nuclei near the valley of β-stability or on neutron-rich nuclei [9,11,16–33]. Experimental data on the OES-FY in neutron-deficient nuclei close to the proton drip line are very scarce mainly due to the very small production cross sections. In addition, full A and Z identification was not achieved in most of the previous experiments (see, e.g., [16,17,20,24,25]). In such cases, the OES-FY can hardly be studied quantitatively. The development of in-flight spectrometers has allowed for both A and Z identification in recent experiments [11,34]. Experimental studies of the OES of light-fragment yields revealed a particularly strong OES for $N = Z$ nuclei, an isospin dependence, and an enhancement of OES when approaching the neutron drip line [11]. These features of the OES-FY are very similar to those observed for the OES of nuclear binding energies (OES-BE) [12,13,35–37], which can be related to nucleon-nucleon pairing correlations [38] and to contributions of the deformed mean field [39]. However, shell effects, which are the most significant and evident feature of the OES-BE, were not observed experimentally for the OES-FY.

There are many theoretical models aimed at explaining the origin of the OES-FY [10,11,28,33]. This OES-FY seems to originate in excited nuclei during the evaporation phase and can be influenced by pairing effects and level densities. But, due to the limited experimental data, a quantitative explanation of this long-standing puzzle about the origin of the OES-FY does not exist. Thus, more experimental studies are needed to profile the evolution of the OES toward drip lines, closed shells, and heavier nuclei. Since the variation of yields over a chain of nuclides with a constant isospin T_z value is rather slow, we study in the following the OES-FY along a constant-T_z chain. This will make the signatures of nuclear structure clear, especially the shell structures.

To make the staggering structure more evident, the magnitude of the local OES-FY for four neighboring fragments centered at $Z + 3/2$ can be quantified using a third-order difference formula [40]:

$$D_{\text{yield}}(Z) = \tfrac{1}{8}(-1)^{Z+1}\{\ln Y(Z+3) - \ln Y(Z) - 3[\ln Y(Z+2) - \ln Y(Z+1)]\}, \quad (1)$$

*hushan@impcas.ac.cn

where $Y(Z)$ is the yield value for the nucleus with a particular value of Z and with a given isospin value T_z. A positive (negative) value of D_{yield} means an enhanced production of even-Z (odd-Z) fragments and a value of zero implies a smooth behavior. The absolute value of D_{yield} indicates the strength of OES.

A combination of an in-flight fragment separator and a storage ring allows for accurate measurements of relative yields of short-lived nuclei produced in fragmentation reactions. Such experimental results can be used to constrain various nuclear reaction models and to study different contributions, such as separation energies and level densities, to the OES-FY. In this work, we present results on the OES of fragment yields obtained by fragmenting relativistic ^{78}Kr projectiles on a beryllium production target. The evolution of the OES-FY of $T_z = -1/2$ and $T_z = 1/2$ nuclei—along or close to the path of αp- and rp-processes near the proton drip line—is studied over a wide range ($A \approx 20$–60), allowing different contributions to the OES-FY due to nuclear structure effects to be disentangled.

II. EXPERIMENTAL DETAILS

The experiment was performed at the experimental Cooler Storage Ring (CSRe) at the Heavy Ion Research Facility in Lanzhou (HIRFL) [41]. After being accelerated and accumulated in the main Cooler Storage Ring (CSRm), a primary beam of ^{78}Kr^{28+} ions at an energy of 482.9 A MeV was directed onto a 15-mm beryllium target placed at the entrance of the second Radioactive Ion Beam Line in Lanzhou (RIBLL2). Neutron-deficient projectile fragments after the target were transmitted through the RIBLL2 and injected into the CSRe. The CSRe was tuned into an isochronous ion-optical mode to enable isochronous mass spectrometry (IMS) [42–45]. The latter was used for accurate measurements of mass-to-charge ratios (m/q) of stored nuclides. The isochronous mode requires the ions to be injected at an energy corresponding to $\gamma = \gamma_t \approx 1.4$, where γ is the relativistic Lorentz factor and γ_t is the transition energy of the CSRe [45,46]. At such high energies, the fragments emerged from the target as fully stripped nuclei. The magnetic rigidity of both the RIBLL2 and the CSRe facilities was fixed to 5.95 Tm in order to achieve the best transmission for the $T_z = -1/2$ nuclides and 6.14 Tm for the $T_z = 1/2$ nuclides of interest.

In the IMS with $\gamma = \gamma_t$, the revolution times of stored ions are the direct measure of their m/q values [45], according to the following relation:

$$\frac{\Delta T}{T} = \frac{1}{\gamma_t{}^2}\frac{\Delta\,(m/q)}{(m/q)}, \tag{2}$$

where T is the revolution time of the ion. A dedicated high-performance time-of-flight detector was developed [47] that allows for accurate revolution time measurement of every stored ion. A time resolution of about 118 ps (full width at half maximum) and a detection efficiency of 20%–70% in one turn, depending on Z of the ions and the number of ions stored simultaneously in the ring, have been achieved for this detector [47]. Signals produced by ions in the detector were recorded by a digital phosphor oscilloscope at a sampling rate of 50 GS/s. The record time was 200 μs per injection, corresponding to about 320 revolutions in each injection for the stored ions with a revolution time of about 616 ns. Thus, a detection efficiency of about 100% was achieved.

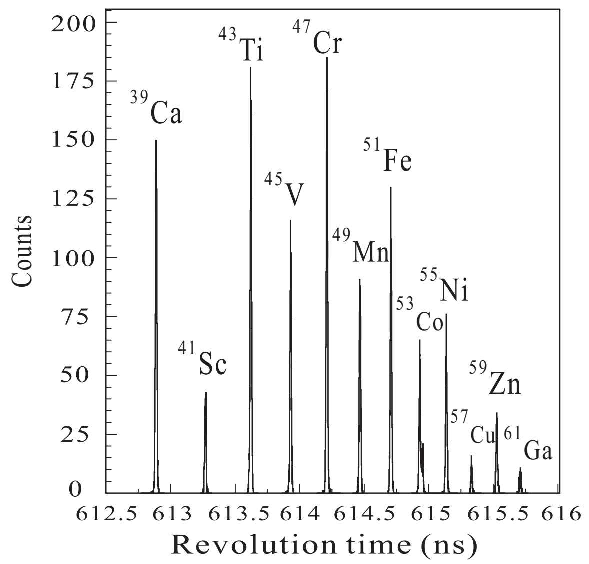

FIG. 1. Part of the measured revolution time spectrum of $T_z = -1/2$ nuclides produced in ^{78}Kr fragmentation reactions on a Be target. Mass and atomic numbers are indicated.

III. DATA ANALYSIS

To determine the revolution time of the nuclides in the ring, the recorded data were analyzed in the same way as described in Refs. [48–51]. Figure 1 shows a part of the measured revolution-time spectrum of $T_z = -1/2$ nuclides. The measured numbers of particles for all of the $T_z = -1/2$ nuclides considered here are greater than 100. A high achieved mass resolving power of $m/\Delta m \approx 170\,000$ enabled unambiguous A and Z identification. However, the resolving power reached did not allow us to resolve the $T_z = 0$ nuclei in this experiment.

The momentum distributions and the transmission efficiencies for various fragments were estimated in a way similar to that described in detail in Refs. [52,53]. The transmission efficiency was estimated by using the LISE++ program [54]. According to the calculations, the transmission efficiency varies almost smoothly with Z along a chain of nuclides with a constant T_z. Decay losses of fragments were neglected, since the half-lives of all considered nuclei are longer than 100 ms, which has to be compared to the acquisition time of merely 200 μs.

IV. RESULTS AND DISCUSSION

A. OES in fragment yields

Figure 2(a) presents the measured yield values corrected for the estimated transmission efficiencies of $T_z = -1/2$ and $T_z = 1/2$ nuclei, which are the yields of these nuclei leaving the target. The OES is very evident for $T_z = -1/2$ nuclides, but it is small for $T_z = 1/2$ nuclides. In the former, the ratio of

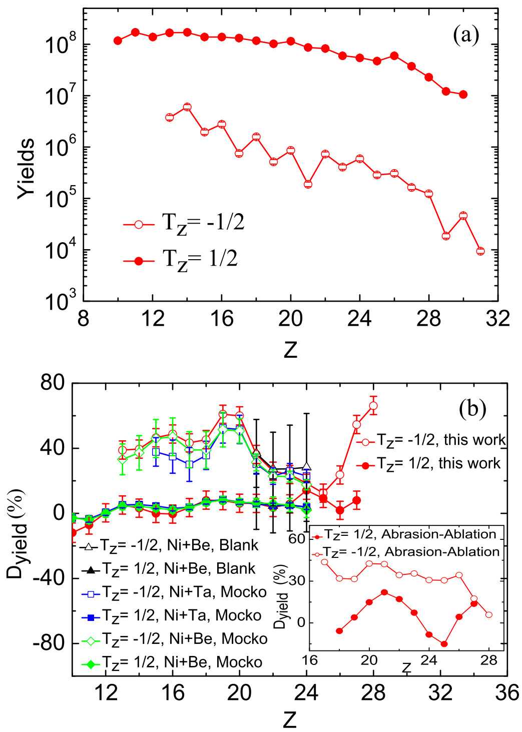

FIG. 2. (Color online) (a) Fragment yields of $T_z = -1/2$ and $T_z = 1/2$ nuclei measured in this experiment. The error of about 10% is dominated by the systematic uncertainty of the estimations of transmission efficiencies [52,53]. (b) The magnitude of the OES-FY for $T_z = -1/2$ and $T_z = 1/2$ nuclei measured in this experiment, and the data from other experiments [15,55], calculated according to Eq. (1). The inset shows the predicted OES-FY for nuclei produced in our experiment by the Abrasion-Ablation model [10], where the parameters are similar to those used in Ref. [53].

the yields of neighboring even- and odd-Z nuclei can reach a factor of 5. A sharp drop of the fragment yields near the closed shells $Z = 20$ and 28 is seen.

The magnitude of the OES for four consecutive yields from our experiment, which is the red point in Fig. 2(b), is calculated by Eq. (1). It is always larger for $T_z = -1/2$ nuclei than for $T_z = 1/2$ nuclei. For the $T_z = -1/2$ nuclei, a significant impact on the OES-FY from the shell structure is observed and the largest D_{yield} value of about 60% is reached near the closed shells $Z = 20$ and 28. The $T_z = 1/2$ nuclei show a very weak OES and there is a transition from reversed OES, with an enhanced production of odd-Z nuclei, to OES at $Z \approx 14$, as shown in Fig. 2. This is in excellent agreement with the results reported in Ref. [11] for $T_z = 1/2$ nuclei with $Z < 20$.

To study the projectile-target dependence of this OES, we also calculate the magnitude of this OES by using Eq. (1), using the reported cross sections from ^{58}Ni + Be reactions in Ref. [15] and the cross sections from ^{58}Ni + Ta reactions and ^{58}Ni + Be reactions in Ref. [55]. For their data, the magnitude of the OES is extracted and studied first by this method. The impact of shell structure on the OES-FY is also evident at the $Z = 20$ shell for the $T_z = -1/2$ nuclei produced in their experiments. For the OES-FY of both $T_z = -1/2$ nuclei and $T_z = 1/2$ nuclei, their data, especially the data from ^{58}Ni + Be reactions, show almost the same evolution tendency as our results. Our experimental results agree well with their data in the low-Z region and thus this OES almost does not depend on the projectile-target combinations within the uncertainties from all these data, as presented in Fig. 2(b).

B. Origin of OES in fragment yields

To our knowledge, no nuclear reaction model can reproduce the above OES-FY over such a wide range, especially for the $T_z = -1/2$ nuclei. For instance, the inset of Fig. 2(b) presents the prediction of the OES-FY for our reactions by using the Abrasion-Ablation model [10]. The evaporation process is simulated by using this model with parameters similar to those used in Ref. [53]. For example, an effective proton evaporation radius [56] of 4 fm and an average excitation energy of about 13 MeV per abraded nucleon are used in the simulation. The separation energies are from the Atomic Mass Evaluation AME'03 [57]; these are in excellent agreement with the latest Atomic Mass Evaluation AME'12 [13] for the nuclei studied in this work. In this model the OES-FY for the $T_z = -1/2$ nuclei is stronger than that for the $T_z = 1/2$ nuclei, but it cannot reproduce the above OES-FY, especially for the shell structures in the OES-FY of the $T_z = -1/2$ nuclei near $Z = 20$ and 28. The discrepancy may come from the choice of parameters in the evaporation model, such as the effective Coulomb barrier parameter, the level density parameters, and the excitation energy.

In the following we will introduce the particle-emission threshold energy (PETE), where all particle decays will cease and the final particle stable fragments will be formed in the evaporation phase [58]. The PETE was proposed to be an important quantity to calculate the fragments yields [10,58,59]. It is the smallest value from either the neutron separation energy (S_n) or the proton separation energy (S_p) of this fragment, which is from the latest Atomic Mass Evaluation AME'12 [13], when there is no other particle stable isomeric states. Indeed, for the case of ^{53}Co, there is a particle stable isomeric state at the excitation energy of $E^* = 3.174$ MeV observed in our experiment, which is higher than $S_p = 1.615$ MeV. This indicates that the particle decays stop at this isomeric state and its excitation energy is the PETE value since it is the observed final particle stable fragment [58]. Figure 3(a) shows the PETE for nuclides with $T_z = -1/2$ and $T_z = 1/2$. For these light nuclei, α-particle emission can be neglected, and the Coulomb barrier, which is a smooth factor and less than 1 MeV for the $Z > 16$ fragments produced in our reactions according to the results in Ref. [60], can also be neglected [58]. The contribution of the γ-ray emission to the OES-FY, which will be studied in detail and reported in a future publication, is also small for these light nuclei. The systematics of PETE values in Fig. 3(a) shows a very similar global tendency and fine structure as the fragment yields in Fig. 2(a), except for the much slower decreasing tendency of PETE than that of fragment yields.

Let us discuss odd-A nuclei. The nuclides measured in this work are close to the proton drip line and will emit predominantly protons. However, due to proton-proton pairing, S_p is large for the even-Z nuclei but small for the odd-Z nuclei.

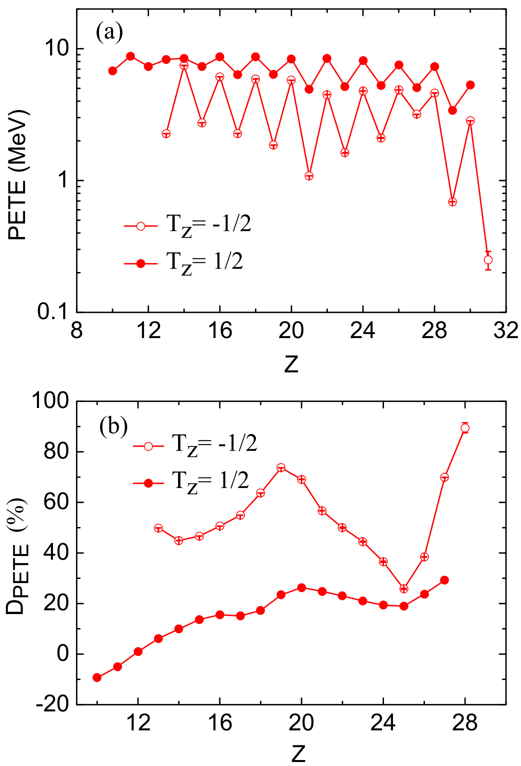

FIG. 3. (Color online) (a) Particle-emission threshold energy for $T_z = -1/2$ and $T_z = 1/2$ nuclei, which equals the lowest value from the neutron- or the proton-separation energy of one particular isotope, except for ^{53}Co, where an isomeric state at an excitation energy of $E^* = 3.174$ MeV was observed as the final particle stable state and this excitation energy is the PETE value. For the PETE, the error bars are less than 1% [13], except for ^{61}Ga. (b) Magnitude of the OES in PETE for $T_z = -1/2$ and $T_z = 1/2$ nuclei, calculated with Eq. (1) and by substituting the yields Y with PETE.

Thus, the yields of these nuclei close to the proton drip line show OES. However, for the $T_z = 1/2$ and $Z \leqslant 14$ nuclei, the situation is opposite. These nuclei will predominantly emit neutrons. S_n is large for the odd-Z (even-N) nuclei but small for the even-Z (odd-N) nuclei due to neutron-neutron pairing. This was also seen for other nuclei closer to the neutron drip line (see Refs. [11,28]). Thus, the yields of these odd-A nuclei close to the neutron drip line should show a reversed OES pattern as compared to nuclei close to the proton drip line. This indicates the evident impact of the proton-proton and neutron-neutron pairing correlations on the PETE and in turn on the OES-FY.

The magnitude of OES in PETE was calculated by using Eq. (1), where the yields Y were replaced by the corresponding PETE values. The obtained results are shown in Fig. 3(b). The OES in PETE and the OES-FY show remarkable similarities: (1) stronger OES for $T_z = -1/2$ nuclei than that for $T_z = 1/2$ nuclei, (2) the strongest OES near the closed shells $Z = 20$ and 28 for $T_z = -1/2$ nuclei, and (3) a transition of OES for $T_z = 1/2$ nuclei from reversed OES to OES at $Z \approx 14$. They present almost the same evolution pattern, as indicated in Figs. 2(b) and 3(b). The above results demonstrated unambiguously that the OES-FY mainly originates from the OES in the minimum

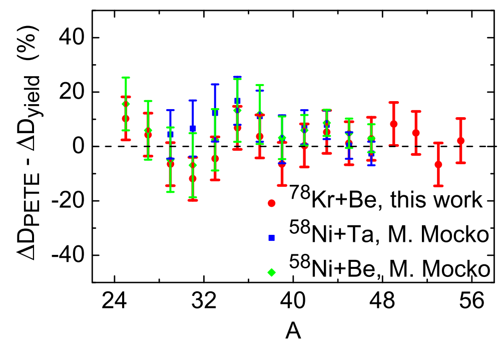

FIG. 4. (Color online) Difference between the relative OES in PETE, $\Delta D_{\rm PETE}(A) = D_{\rm PETE}(A, T_z = -1/2) - D_{\rm PETE}(A, T_z = 1/2)$, and the relative OES-FY $\Delta D_{\rm yield}(A) = D_{\rm yield}(A, T_z = -1/2) - D_{\rm yield}(A, T_z = 1/2)$ for mirror nuclei measured in our experiment, and the data from other experiments [55].

value of S_n and S_p, which are strongly affected by both pairing and shell effects. However, the OES-FY is slightly weaker than the OES in PETE, as presented in Figs. 2(b) and 3(b). One possible reason for this is that the influence of the level densities on the OES-FY is not yet considered [10,11,33,58].

Since the dependence of level density on isospin is weak [58], and mirror nuclei with the same A measured in our experiment have very similar level structure, the contribution of level densities to the relative OES-FY of these mirror nuclei will almost be negligible. Therefore, we plot in Fig. 4 the difference of the relative OES in PETE, $\Delta D_{\rm PETE}(A) = D_{\rm PETE}(A, T_z = -1/2) - D_{\rm PETE}(A, T_z = 1/2)$, and the relative OES-FY $\Delta D_{\rm yield}(A) = D_{\rm yield}(A, T_z = -1/2) - D_{\rm yield}(A, T_z = 1/2)$ of mirror nuclei. A striking observation is that the relative OES is almost the same and $\Delta D_{\rm PETE}(A) - \Delta D_{\rm yield}(A) \approx 0$. Both the new results from our experiment and the OES-FY extracted from other experiments [55] with different projectile-target combinations support this observation. A small local deviation near $A = 31$, although compatible with the statistical 1σ uncertainties, may come from the Coulomb barrier difference for nuclides with different particle (neutron or proton) emission around the transition area. For these mirror nuclei, the results quantitatively prove that the origin of the OES-FY is mainly from OES in PETE.

All of the above results can be explained with the theory of Campi and Hüfner [58]. The isobaric and isotopic yields are dominated by the phase space (level density) of the final particle stable fragment at its PETE in the evaporation phase. Both our experimental results and the data from other experiments [55] strongly support the theory that the OES-FY is dominated by the OES in PETE, where the influences of both pairing correlations and prominent shell effects are clearly observed.

V. SUMMARY

In summary, we have measured the fragments yields of $T_z = -1/2$ and $T_z = 1/2$ nuclei, over a wide range of mass numbers, produced by ^{78}Kr fragmentation on a Be target at an energy of 482.9 A MeV. The OES-FY is very strong for $T_z = -1/2$ nuclides but weak for $T_z = 1/2$ nuclides. The significant impact of both pairing and shell structure, especially at the closed shells $Z = 20$ and 28, on the deduced OES-FY is observed.

The OES in PETE was also investigated quantitatively. Striking similarities are demonstrated between the OES-FY and the OES in PETE. The measured OES-FY for the $T_z = -1/2$ and $T_z = 1/2$ mirror nuclei allowed us to compare the relative OES-FY and the relative OES in PETE of mirror nuclei. The comparison proved that the origin of OES-FY is mainly due to the OES in PETE, where the strong impact of both nuclear pairing and shell structure exists.

ACKNOWLEDGMENTS

We thank Dr. A. Stolz and Dr. T. Baumann for their help on the LISE++ program. This research was partially supported by the 973 Program of China (No. 2013CB834401), by a BMBF grant in the framework of the Internationale Zusammenarbeit in Bildung und Forschung (Project No. 01DO12012), by the Helmholtz–CAS Joint Research Group (HCJRG-108), by the External Cooperation Program of the Chinese Academy of Sciences (Grant No. GJHZ1305), by the Max-Planck Society, by the joint Max Planck/CAS doctoral promotion program, by the ESF through the EuroGENESIS program, by the HGF Young Investigators Project No. VH-NG-327, by the National Natural Science Foundation of China (Grants No. 10925526, No. 11035007, No, U1232208, No. 10675147, No. 10805059, No. 11135005, No. 11075103, and No. 11205205), and by the Chinese Academy of Sciences through the visiting professorship for senior international scientists program (Grant No. 2009J2-23).

[1] C. E. Rolfs and W. S. Rodney, *Cauldrons in the Cosmos* (University of Chicago Press, Chicago, 1988).
[2] T. Rauscher, F. K. Thielemann, and K. L. Kratz, Phys. Rev. C **56**, 1613 (1997).
[3] A. Aprahamian, K. Langanke, and M. Wiescher, Prog. Part. Nucl. Phys. **54**, 535 (2005).
[4] O. B. Tarasov *et al.*, Phys. Rev. Lett. **102**, 142501 (2009).
[5] O. B. Tarasov *et al.*, Phys. Rev. C **87**, 054612 (2013).
[6] F. Wienholtz *et al.*, Nature (London) **498**, 346 (2013).
[7] D. Steppenbeck *et al.*, Nature (London) **502**, 207 (2013).
[8] T. Otsuka, T. Suzuki, M. Honma, Y. Utsuno, N. Tsunoda, K. Tsukiyama, and M. Hjorth-Jensen, Phys. Rev. Lett. **104**, 012501 (2010).
[9] K. Hagino and H. Sagawa, Phys. Rev. C **85**, 037604 (2012).
[10] J. J. Gaimard and K. H. Schmidt, Nucl. Phys. A **531**, 709 (1991).
[11] M. V. Ricciardi *et al.*, Nucl. Phys. A **733**, 299 (2004).
[12] W. Heisenberg, Z. Phys. **78**, 156 (1932).
[13] M. Wang *et al.*, Chin. Phys. C **36**, 1603 (2012).
[14] B. Cheal and K. T. Flanagan, J. Phys. G: Nucl. Part. Phys. **37**, 113101 (2010).
[15] B. Blank *et al.*, Phys. Rev. C **50**, 2398 (1994).
[16] C. N. Knott *et al.*, Phys. Rev. C **53**, 347 (1996).
[17] C. Zeitlin *et al.*, Phys. Rev. C **56**, 388 (1997).
[18] C. N. Knott *et al.*, Phys. Rev. C **56**, 398 (1997).
[19] C. X. Chen *et al.*, Phys. Rev. C **56**, 1536 (1997).
[20] L. B. Yang *et al.*, Phys. Rev. C **60**, 041602(R) (1999).
[21] E. M. Winchester *et al.*, Phys. Rev. C **63**, 014601 (2000).
[22] A. Leistenschneider *et al.*, Phys. Rev. C **65**, 064607 (2002).
[23] E. Geraci *et al.*, Nucl. Phys. A **732**, 173 (2004).
[24] G. Iancu, F. Flesch, and W. Heinrich, Radiat. Meas. **39**, 525 (2005).
[25] C. Zeitlin *et al.*, Phys. Rev. C **77**, 034605 (2008).
[26] M. Huang *et al.*, Phys. Rev. C **81**, 044620 (2010).
[27] M. Huang *et al.*, Phys. Rev. C **82**, 054602 (2010).
[28] M. V. Ricciardi, K. H. Schmidt, and A. Kelić-Heil, arXiv:1007.0386.
[29] J. Su, F.-S. Zhang, and B.-A. Bian, Phys. Rev. C **83**, 014608 (2011).
[30] I. Lombardo *et al.*, Phys. Rev. C **84**, 024613 (2011).
[31] M. D'Agostino *et al.*, Nucl. Phys. A **861**, 47 (2011).
[32] G. Casini *et al.*, Phys. Rev. C **86**, 011602(R) (2012).
[33] M. D'Agostino *et al.*, Nucl. Phys. A **875**, 139 (2012).
[34] J. R. Winkelbauer, S. R. Souza, and M. B. Tsang, Phys. Rev. C **88**, 044613 (2013).
[35] Y. Litvinov *et al.*, Phys. Rev. Lett. **95**, 042501 (2005).
[36] B. Jurado *et al.*, Phys. Lett. B **649**, 43 (2007).
[37] J. Hakala *et al.*, Phys. Rev. Lett. **109**, 032501 (2012).
[38] A. Bohr and B. R. Mottelson, *Nuclear Structure* (World Scientific, Singapore, 1998).
[39] W. Satula, J. Dobaczewski, and W. Nazarewicz, Phys. Rev. Lett. **81**, 3599 (1998).
[40] B. L. Tracy *et al.*, Phys. Rev. C **5**, 222 (1972).
[41] J. W. Xia *et al.*, Nucl. Instrum. Methods A **488**, 11 (2002).
[42] M. Hausmann *et al.*, Nucl. Instrum. Methods A **446**, 569 (2000).
[43] M. Hausmann *et al.*, Hyperfine Interact. **132**, 289 (2001).
[44] B. Sun *et al.*, Nucl. Phys. A **812**, 1 (2008).
[45] B. Franzke, H. Geissel, and G. Münzenberg, Mass Spectrom. Rev. **27**, 428 (2008).
[46] F. Bosch, Y. A. Litvinov, and T. Stöhlker, Prog. Part. Nucl. Phys. **73**, 84 (2013).
[47] B. Mei *et al.*, Nucl. Instrum. Methods A **624**, 109 (2010).
[48] X. L. Tu *et al.*, Phys. Rev. Lett. **106**, 112501 (2011).
[49] X. L. Tu *et al.*, Nucl. Instrum. Methods A **654**, 213 (2011).
[50] Y. H. Zhang *et al.*, Phys. Rev. Lett. **109**, 102501 (2012).
[51] X. L. Yan *et al.*, Astrophys. J. Lett. **766**, L8 (2013).
[52] J. Kurcewicz *et al.*, Phys. Lett. B **717**, 371 (2012).
[53] T. Yamaguchi *et al.*, Phys. Rev. C **74**, 044608 (2006).
[54] O. Tarasov and D. Bazin, Nucl. Instrum. Methods B **266**, 4657 (2008).
[55] M. Mocko *et al.*, Phys. Rev. C **74**, 054612 (2006).
[56] J. Benlliure *et al.*, Eur. Phys. J. A **2**, 193 (1998).
[57] G. Audi, A. H. Wapstra, and C. Thibault, Nucl. Phys. A **729**, 337 (2003).
[58] X. Campi and J. Hüfner, Phys. Rev. C **24**, 2199 (1981).
[59] J. Hüfner, C. Sander, and G. Wolschin, Phys. Lett. B **73**, 289 (1978).
[60] A. S. Hirsch *et al.*, Phys. Rev. C **29**, 508 (1984).